

## Structure of self-interstitial atom clusters in iron and copper

Akiyuki Takahashi<sup>1</sup> and Nasr M. Ghoniem<sup>2</sup><sup>1</sup>*Department of Mechanical Engineering, Faculty of Science and Technology, Tokyo University of Science, 2641 Yamazaki, Noda-shi, Chiba 278-8510, Japan*<sup>2</sup>*Department of Mechanical and Aerospace Engineering, University of California–Los Angeles, Los Angeles, California 90095, USA*  
(Received 5 December 2008; revised manuscript received 15 October 2009; published 5 November 2009)

The dislocation core structure of self-interstitial atom (SIA) clusters in bcc iron and fcc copper is determined using the hybrid *ab initio* continuum method of Banerjee *et al.* [Philos. Mag. **87**, 4131 (2007)]. To reduce reliance on empirical potentials and to facilitate predictions of the effects of local chemistry and stress on the structure of defects, we present here a hybrid extension of the Peierls-Nabarro continuum model, with lattice resistance to slip determined separately from *ab initio* calculations. A method is developed to reconstruct atomic arrangements and geometry of SIA clusters from the hybrid model. The results are shown to compare well with molecular-dynamics simulations. In iron, the core structure does not show dependence on the size of the self-interstitial cluster, and is nearly identical to that of a straight edge dislocation. However, the core structure of SIA clusters in Cu is shown to depend strongly on the cluster size. Small SIA clusters are found to have nondissociated compact dislocation cores, with a strong merging of Shockley partial dislocations and a relatively narrow stacking fault (SF) region. The compact nature of the SIA core in copper is attributed to the strong dependence of the self-energy on the cluster size. As the number of atoms in the SIA cluster increases, Shockley partial dislocations separate and the SF region widens, rendering the SIA core structure to that of an edge dislocation. The separation distance between the two partials widens as the cluster size increases, and tends to the value of a straight edge dislocation for cluster sizes above 400 atoms. The local stress is found to have a significant effect on the atomic arrangements within SIA clusters in copper and the width of the stacking faults. An applied external shear can delocalize the core of an SIA cluster in copper, with positive shear defined to be on the (111) plane along the  $[\bar{1}\bar{1}2]$  direction. For an SIA cluster containing 1600 atoms, a positive 1 GPa shear stress delocalizes the cluster and expands the SF to  $30b$ , while a negative shear stress of 2 GPa contracts the core to less than  $5b$ , where  $b$  is the Burgers vector magnitude.

DOI: [10.1103/PhysRevB.80.174104](https://doi.org/10.1103/PhysRevB.80.174104)

PACS number(s): 61.72.Bb, 61.80.Az, 61.72.Nn

### I. INTRODUCTION

During energetic particle interaction with crystalline solids, self-interstitial atoms (SIA) readily aggregate in the near vicinity of collision cascades initiated by energetic ions or neutrons, and they cluster into tightly bound coherent configurations known as self-interstitial atom clusters.<sup>1,2</sup> Such clusters tend to move in tightly bound configurations along crystallographic orientations with the highest atomic density, and occasionally change their directions of motion in response to temperature fluctuations or stress inhomogeneities.<sup>3</sup> The one-dimensional nature of SIA cluster diffusion has been shown to result in a variety of important consequences in irradiated materials, such as the alignment of imperfect void and bubble lattices,<sup>4</sup> the emergence of spatially ordered dislocation structures,<sup>5,6</sup> and the modification of the order of reaction kinetics in rate theory models.<sup>7</sup> SIA clusters have also been investigated for their influence on the strength and ductility of irradiated materials.<sup>8–11</sup>

To understand the contribution of SIA clusters to the variety of phenomena associated with radiation interaction with materials, it is essential to address the fundamental physics of these defects. The geometry of atomic arrangements of SIA clusters often controls their interactions with the microstructure, and hence should be accurately determined. SIA clusters are defects that can be regarded as small dislocation loops. However, since they are so small, application of dislocation theory to describe their elastic interactions may be

questionable, because the elastic theory of defects ignores the structure of the dislocation core. Another more realistic approach to studies of SIA cluster interactions with other defects is the molecular-dynamics (MD) simulation method. MD simulations were performed in order to understand the detailed mechanisms of the dynamical interactions between SIA clusters and other defects. For example, Osetsky *et al.*<sup>3</sup> performed MD simulations of the interaction between an edge dislocation and an SIA cluster in bcc iron and fcc copper. They studied the influence of SIA clusters on the dynamics of dislocations, and discussed the possible effects of dislocation decoration by SIA clusters on radiation hardening. Bacon *et al.*<sup>12</sup> performed MD simulations of the interaction between an edge dislocation and a self-interstitial loop in bcc iron, and described the atomistic mechanism of the formation of a super jog on the dislocation line as a result of its interaction with the SIA cluster. However, MD simulation results must be carefully interpreted for direct quantitative information, because the reliability of the results strongly depends on the accuracy of underlying empirical interatomic potentials. A recent interesting example reveals that while MD simulations utilizing the embedded atom method predict that dislocations in Al dissociate into partials,<sup>13</sup> no such dissociation was ever observed experimentally.<sup>14</sup> Also, the spreading of the Lomer dislocation predicted by the Voter-Chen potential for aluminum is not experimentally observed, and the Ercolessi-Adams potential does not accurately model the

dissociation of the  $60^\circ$  dislocation in aluminum.<sup>15</sup> Presently, MD simulations of dislocation properties and interactions are also limited to mostly straight dislocations with simplified boundary conditions. Alternatively, *ab initio* calculations are considered to be more reliable for quantitative predictions of defect properties.<sup>16,17</sup> Nevertheless, direct applications of *ab initio* methods to defect problems is very challenging, because of severe computational limitations on the number of atoms within a simulation cell.

One of the most successful defect models is that due to Peierls and Nabarro, in which the dislocation core structure is atomistically resolved on the basis of the continuum theory of elasticity.<sup>18</sup> In the Peierls-Nabarro (PN) model, the core structure is determined by balancing the crystal lattice restoring forces with elastic interactions between infinitesimal incompatibilities (dislocations) within the dislocation core. The model relies on the decomposition of the problem into two components. Large atomic displacements associated with “slip” are localized on the slip plane, and are treated as material incompatibilities. The interaction between atoms in the remainder of the crystal is obtained using the theory of elasticity. The original PN model is restricted to the analysis of the cores of infinitely long and straight dislocations, and utilizes assumed lattice resistance forces arising from the displacement of one part of the crystal relative to the other across the slip plane. Recently, Banerjee *et al.*<sup>19</sup> proposed an atomistic-continuum hybrid computational method that extends the original PN model to dislocation problems of arbitrarily complex shape, and that directly utilizes *ab initio* information to reconstruct lattice restoring forces. The balance equations in the extended PN model are solved using the parametric dislocation dynamics (PDD) approach.<sup>20,21</sup> The lattice restoring stress in the PN model is determined with *ab initio* density-functional theory (DFT) in the form of generalized stacking fault (GSF) energy.<sup>22</sup> The method has been successfully applied to studies of the core structure of shear dislocation loops,<sup>19</sup> and to dislocation transmission across the interface of elastic bimetals.<sup>23</sup>

The present study has two objectives. The first objective is to advance the development of the hybrid atomistic-continuum method of Banerjee *et al.*, extending it to the determination of the core structure of SIA clusters. We investigate here the dependence of the core structure of SIA clusters on their sizes, and on the local stress environment in Fe (bcc) and Cu (fcc). The second objective is to elucidate the influence of applied stress on the atomic structure of SIA clusters and to reveal the conditions for drastic deviations from unstressed configurations. In particular, we wish to find out the magnitude and nature of the local stress that results in compacting dissociated SIA cores in copper, and in addition, in delocalizing the core completely.

While straight and infinitely long dislocations have no self-forces associated with them, small dislocation loops possess strong self-forces that are expected to influence atomic displacements within the core. Such self-force effects can be important if their magnitude is comparable to the lattice restoring forces. The distribution of these forces on the slip plane can result in a compact core, as in the case of Fe, or a

dissociated core, as in Cu. The interference of strong self-forces with this force structure is thus expected to change the core structure of small SIA dislocation loops. We will examine here this delicate balance, which is a function of the cluster size and the local stress environment. In order to make detailed atomistic investigations of the dislocation core, we present a distinct method for reconstruction of atomic arrangements directly from the hybrid *ab initio* continuum model. Using this method, the atomic arrangements of SIA clusters will be calculated and compared to the results of classical MD simulations. Finally, we will show that SIA clusters in copper respond to an applied shear stress by adjusting their core sizes and atomic displacements within.

In the following, we first present detail of the present computational method in Sec. II, including a discussion of our method of deriving atomic positions from the model. This is followed by the results for the core structure of SIA clusters in Fe and Cu, presented in Sec. III. The influence of an externally applied shear stress on the core structure of SIA clusters in Cu is discussed in Sec. IV, while a summary and conclusions are finally given in Sec. V.

## II. COMPUTATIONAL METHOD

Banerjee *et al.*<sup>19</sup> proposed a hybrid *ab initio* continuum method to enable determination of the core structure of dislocations of arbitrarily complex geometry. The approach is an extension of the original Peierls-Nabarro model,<sup>18</sup> in which a balance is sought between forces arising from infinitesimal displacements within the dislocation core and lattice restoring forces. This balance can be expressed as

$$p(x) = \frac{\mu}{\pi(1-\nu)} \int_{-\infty}^{\infty} \frac{1}{x' - x} \frac{du}{dx'} dx', \quad (1)$$

where,  $p(x)$  is the lattice restoring force,  $\mu$  and  $\nu$  are the elastic shear modulus and Poisson’s ratio, respectively,  $x$  is the position of an infinitesimal element of displacement where the force balance in Eq. (1) is evaluated, while  $x'$  is the position of any other infinitesimal element of displacement, and  $u$  is the sought-after atomic displacement within the dislocation core. To numerically solve Eq. (2), the dislocation core is first discretized into a number ( $N$ ) of infinitesimal dislocations, and the Burgers vector of each infinitesimal dislocation is set to  $b/N$  to keep the total displacement of the dislocations. The equivalent discrete form of Eq. (2) then takes the form

$$p(x_i) = \frac{\mu}{\pi(1-\nu)} \frac{b}{2N} \sum_{j \neq i}^N \frac{1}{x_j - x_i}. \quad (2)$$

The elastic interaction term between displacements in the dislocation core in Eq. (2) can be replaced with an elastic interaction between infinitesimal dislocations. Thus, Eq. (2) can be solved for a dislocation of complex three-dimensional geometry using the methodology of parametric dislocation dynamics.<sup>20,21</sup> The original PN model is modified in two respects: (1) the lattice restoring force term on the left-hand side of Eq. (2) is calculated utilizing modern computational

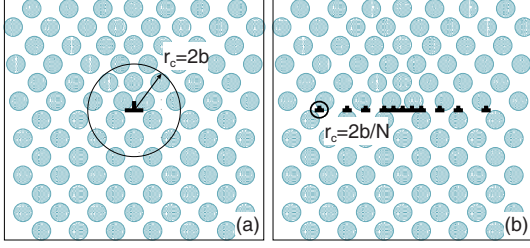


FIG. 1. (Color online) Dislocation core region of (a) a perfect dislocation and (b) each infinitesimal dislocation.

quantum mechanics,<sup>24</sup> and (2) the applied and self-stress (for curved dislocations) are added to the lattice restoring force. The gradient of the orientation-dependent slip energy, known as the generalized stacking fault energy, or the  $\gamma$  surface, is used to determine  $p$ .

$$p = -\frac{d\gamma}{du},$$

where,  $\gamma$  is the energy required to rigidly displace two crystal halves, cut along the slip plane, in a specified direction. We compute this energy surface using density-functional theory, implemented within the VASP *ab initio* computer program.<sup>25</sup> Thus, the lattice restoring stress contains information on the atomistic stacking fault structure and works as a bridge between atomistic and continuum formulations. The total stress on infinitesimal dislocations in PDD simulations is then given by

$$\sigma_{total} = \sigma_{self} + \sigma_{PK} + \sigma_{fric} + p,$$

where  $\sigma_{self}$  is the self-stress,  $\sigma_{PK}$  is the elastic interaction stress between infinitesimal dislocations, and  $\sigma_{fric}$  is the friction stress.

The results of hybrid simulations are the positions of infinitesimal dislocations and the distribution of displacements within the dislocation core. Although such information is very useful in understanding the core structure of a particular dislocation, atomic configurations should provide a more physical picture. To study the atomic arrangements within the dislocation core and hence make direct comparisons with MD results, we develop here a distinct method for the reconstruction of atomic positions in a crystal that contains a dislocation. The displacement field around a dislocation is known to be accurate up to a distance of around  $2b$  from the dislocation. Since infinitesimal dislocations in our hybrid method have very small Burgers vector,  $b/N$ , calculations of atomic displacements within the core should be accurate up to a distance of  $\sim 2b/N$  from the center of each infinitesimal dislocation (see Fig. 1). For example, if 20 infinitesimal dislocations were used to describe a dislocation core, atomic displacements are accurate to within a distance of  $\sim b/10$  from the center of each infinitesimal dislocation. The accuracy can be increased if we use more infinitesimal dislocations. Ghoniem and Sun<sup>26</sup> developed a fast-sum method to calculate the elastic stress, strain and displacement of curved dislocations numerically and accurately. The equation to calculate displacements caused by dislocation loops is given by

$$u_i = \frac{1}{4\pi} \sum_{\gamma=1}^{N_{loop}} \left[ -b_i \Omega + \frac{1}{2} \sum_{\beta=1}^{N_s} \sum_{\alpha=1}^{Q_{max}} w_{\alpha} \right. \\ \left. \times \left( \epsilon_{ikl} b_l R_{,pp} + \frac{\epsilon_{kmn} b_n R_{,mij}}{1-\nu} \right) \hat{x}_{k,u} \right],$$

where,  $N_{loop}$  is the number of dislocation loops,  $\Omega$  is the solid angle,  $N_s$  is the number of segments in the dislocation loop,  $Q_{max}$ ,  $u$ , and  $w_{\alpha}$  are the number of integral points, the normalized coordinate of the integral point, and the weight function for the Gauss numerical integration, respectively. In the construction of atomic arrangements based on elasticity, an atomic volume is first prepared. Then, infinitesimal dislocations are placed into the atomic volume. Equation (2) is integrated to calculate the displacement field of the  $N$  infinitesimal dislocations at each atomic site, and all atoms are displaced from their perfect-crystal sites by a vector given in Eq. (2).

### III. CORE STRUCTURE OF SELF-INTERSTITIAL ATOM CLUSTERS

The arrangement of atoms participating in SIA clusters has been revealed by a number of researchers, mainly using the classical MD method. Osetsky *et al.*<sup>27</sup> studied the core structure and binding energies of self-interstitial loops in bcc iron and fcc copper using two types of interatomic potentials and discussed energetically stable configurations in different orientations, and the dependence of the structure on the loop size. Kuramoto *et al.*<sup>28</sup> also evaluated the core structure of self-interstitial loops in bcc iron with a Finnis-Sinclair interatomic potential, studied energetically stable structures, and proposed a mechanism for their motion. In this section, we present results for the core structure of self-interstitial loops in bcc iron and fcc copper using the *ab initio* continuum hybrid method. We explore two main aspects here: the dependence of the core structure on the loop size, and the influence of an externally applied stress on the SIA core. The results of the present method will also be directly compared to MD simulations.

#### A. Self-interstitial clusters in iron

In the studies of Osetsky *et al.*, the most stable SIA clusters in Fe were found to be sets of parallel  $\langle 111 \rangle$  crowdions, and that large clusters form perfect dislocation loops with Burgers vector  $\mathbf{b} = \frac{1}{2}\langle 111 \rangle$ . Small clusters of  $\langle 100 \rangle$  crowdions were found to transform into a set of  $\langle 111 \rangle$  crowdions on annealing, while larger clusters (having more than nine SIAs) were found to be stable and form perfect dislocation loops with  $\mathbf{b} = \langle 100 \rangle$ . We consider here the self-interstitial loop geometry shown in Fig. 2 as a representation of a cluster of parallel  $\langle 111 \rangle$  crowdions.<sup>27</sup> The self-interstitial loop has a hexahedral shape, and all straight segments in the loop can glide on their own slip plane such as  $(\bar{1}10)$ ,  $(\bar{1}01)$ , and  $(0\bar{1}1)$ . The Burgers vector of all segments is  $a_0/2[111]$ , where  $a_0$  is the lattice constant of bcc iron (0.28665 nm). We consider prismatic dislocation loops containing SIAs of 91,

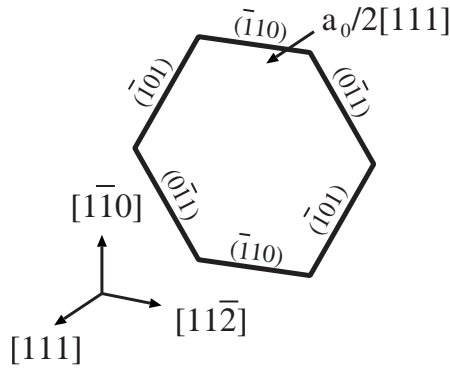


FIG. 2. Geometry of self-interstitial dislocation loops in iron simulated by the hybrid method.

397, and 919 to study the dependence on the size and conform with the hexagonal shape of the loop. The present study is aimed at understanding the core structure of dislocation loops and not the determination of their equilibrium shapes. As such, the equilibrium shape of the loop on its habit plane follows from independent MD calculations,<sup>27</sup> and only the out-of-plane deformation associated with its core structure is analyzed. The in-plane shape of the loop may deviate from its initial predetermined configuration and in highly anisotropic materials may require the utilization of the full anisotropic theory of elasticity. Such developments are outside the scope of the present study and may warrant future efforts.

First, a benchmark computation was performed to determine the accuracy of the hybrid method to represent the core structure of a straight edge dislocation in bcc iron with different numbers of infinitesimal dislocations (e.g., 5, 10, 15, and 20). The results of the benchmark test indicate that more than ten infinitesimal dislocations are needed to calculate the core structure accurately. Thus, in all subsequent calculations of the core structure of self-interstitial loops, we use 20 infinitesimal dislocations.

The GSF energy of iron along the Burgers vector direction of  $\langle 111 \rangle$  on a  $\{110\}$  glide plane is calculated by the *ab initio* method so as to determine the lattice restoring stress in Fe. The calculated dependence of the GSF energy on displacement is shown in Fig. 3. To facilitate calculations of the lattice restoring stress, the GSF energy,  $E_{\text{GSF}}$ , is fitted to an analytical equation of the form

$$E_{\text{GSF}} = E_0 + \left( \frac{A}{W\sqrt{\pi/2}} \right) \exp \left[ -2 \left( \frac{u - u_c}{W} \right)^2 \right],$$

where,  $E_0$ ,  $A$ ,  $W$ , and  $u_c$  are the fitting parameters, having the values of:  $-0.0110$ ,  $0.118$ ,  $1.26397$ , and  $1.241$ , respectively. Taking the derivative of  $E_{\text{GSF}}$  with respect to  $u$ , the lattice restoring stress can be evaluated and used in hybrid simulations.

Figure 4 shows the results of the present method for the core structure of self-interstitial loops in iron. In the figure, infinitesimal dislocation arrays representing SIA clusters containing 91, 397, and 919 SIAs are approximately self-similar, and form very compact dislocation cores. Although the results for the equilibrium positions of infinitesimal ar-

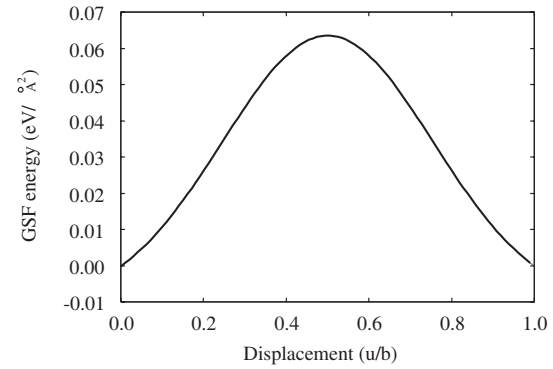


FIG. 3. GSF energy of bcc iron along the  $(110)$  plane in the  $[111]$  direction. The displacement  $u$  is normalized by the Burgers vector magnitude,  $b$ .

rays show the macroscopic shape and core structure of the loops, the atomic arrangement around the core is also of interest. To study the atomic arrangement within the core of such SIA loops we performed classical MD simulations for a loop containing 91 SIAs, using the interatomic potentials for iron developed by Finnis and Sinclair<sup>29</sup> and by Mendelev *et al.*<sup>30</sup> In MD simulations, we set up an atomic volume with a size of  $5.7 \times 5.7 \times 5.7 \text{ nm}^3$ . A hexahedral shape of  $(111)$  extra atomic plane with 91 atoms is placed at the center of the atomic volume. Numerical quenching is performed to determine the stable configuration of the self-interstitial loop when the potential energy of the atomic system converges to a constant.

Figure 5 shows two-dimensional views of atomic arrangements in the vicinity of the dislocation core of a 91-atom SIA cluster. In the figure, atomic positions are shown on the  $(11\bar{2})$  plane, which intersects perpendicularly two straight segments of the loop. It is clear that atomic arrangements obtained by MD simulations are nearly identical, and that they are the same as those obtained with the present method. The dislocation loop core spreads only into a very narrow region of about  $6b$ , indicating that both interatomic potentials give the same edge dislocation core structure. The atomic arrangements indicate that the core of iron SIA clusters calculated by the present method is also compact and is very similar to the core structure obtained by the two interatomic potentials. It is worth noting that the construction of atomic arrangements from the results of the hybrid method is shown to be very useful in detailed comparisons with MD simulations.

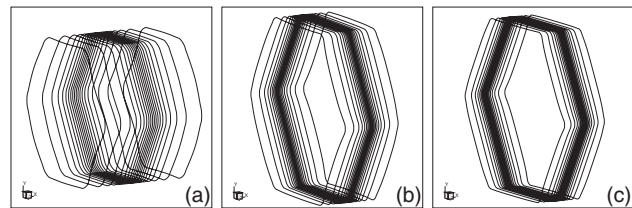


FIG. 4. Core structure of self-interstitial loops containing (a) 91, (b) 397, and (c) 919 SIAs in iron. Each line represents one infinitesimal dislocation loop and is also considered as an equidistance contour line incremented by  $b/20$  ( $\sim 0.014 \text{ nm}$ ).

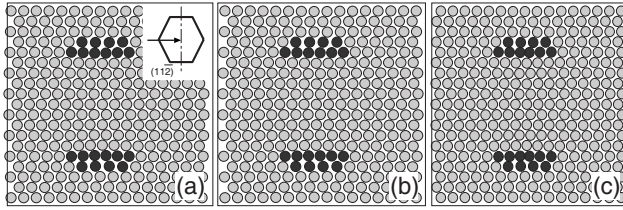


FIG. 5. Atomic arrangement of a 91-atom SIA loop on the  $(11\bar{2})$  plane in iron obtained by MD simulations with interatomic potentials developed by (a) Finnis and Sinclair and (b) Mendeleev *et al.* Results of the present method are shown in (c). The colors are based on the coordination number, where filled black circles have a coordination number different from (8).

The dependence of the core structure on the size of the loop is shown in Fig. 6, where the displacement distributions in the dislocation core of SIA loops are shown for various sizes. For comparison, we also plot the results of hybrid simulations for a straight edge dislocation. It can be observed that the displacements are concentrated within a width of  $6b$ , and that the core structure (i.e., displacement distribution) is identical in all loops. Moreover, the core structures of an SIA loop in Fe is the same as that of a straight edge dislocation. We also plot the displacement density in the dislocation core, which is calculated by taking the derivative of the displacement in the dislocation core with respect to the coordinate along the Burgers vector direction, as shown in Fig. 7. The figure shows that the displacement density in all SIA loops is nearly size independent, and shows a very sharp peak at the center of the dislocation core. The strong lattice restoring forces here (gradients of the rising part of the GSF energy curve in Fig. 3) result in a very compact dislocation core of SIA loops in Fe regardless of their sizes (or self-energies).

**B. Self-interstitial clusters in copper**

Osetsky *et al.* performed MD simulations of SIA clusters containing up to 127 interstitials and found that the most stable configurations are rhombus pure edge loops  $\frac{1}{2}\langle 110 \rangle \{110\}$  and hexagonal Frank loops  $\frac{1}{3}\langle 111 \rangle \{111\}$ . Since the possibility of dissociation into Shockley partial disloca-

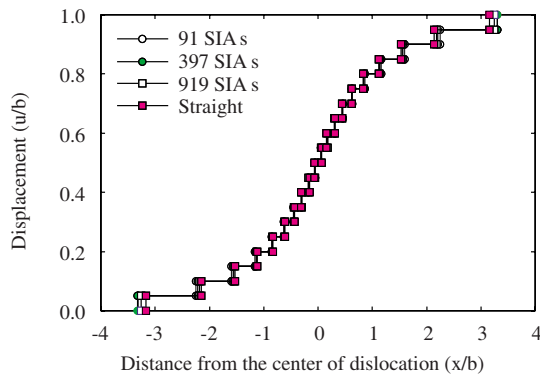


FIG. 6. (Color online) Displacement distribution of the self-interstitial dislocation loop core in iron. The displacement distribution of a straight edge dislocation is also plotted.

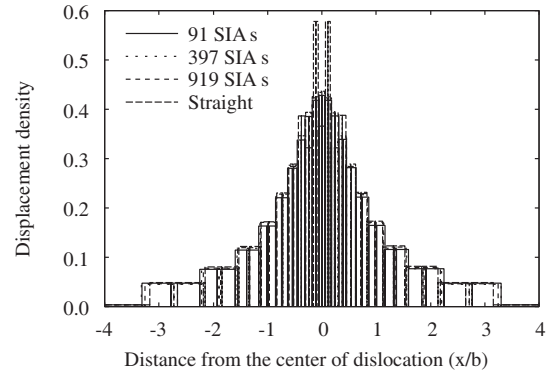


FIG. 7. Displacement density distribution of the self-interstitial dislocation loop core in iron. The displacement density distribution of a straight edge dislocation is also plotted.

tions exists for copper, we consider SIA loops of a rhombus shape, with each segment on a slip plane, such as  $(111)$  and  $(11\bar{1})$ , as shown in Fig. 8. The interatomic potentials developed by Ackland *et al.* and by Mishin *et al.* provide the stacking fault energies of 36.0 and 44.4 mJ/m<sup>2</sup>, respectively. Early measurements of the SF energy in copper are based on a variety of techniques, with values showing considerable variations.<sup>31</sup> The value measured by Pande<sup>31</sup> was reported as  $94 \pm 30$  mJ/m<sup>2</sup> is less reliable, because it was obtained indirectly by the extrapolation from measurements on Cu-Al alloys.<sup>31</sup> More direct measurements based on the dissociation

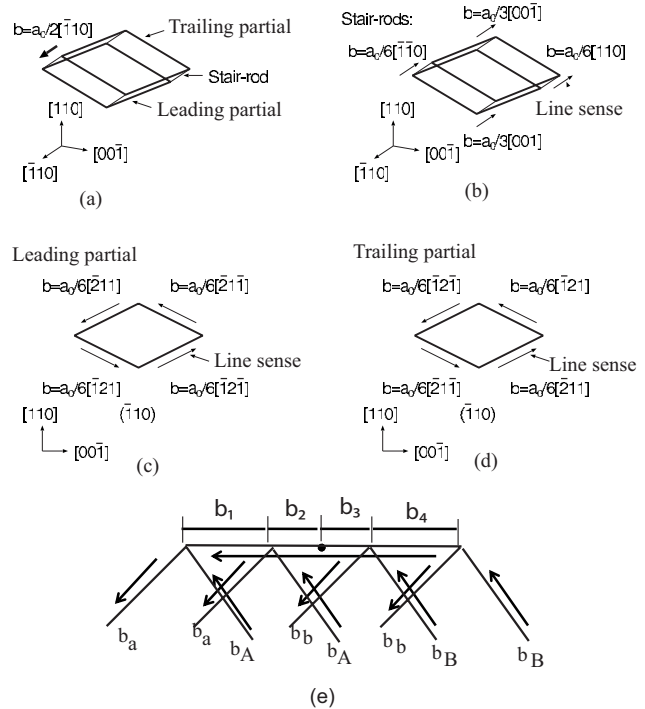


FIG. 8. Geometry of SIA cluster modeled as a rhombus-shaped edge dislocation loop in copper simulated by the hybrid method. (a) Burgers vector of the full prismatic loop; (b) stair-rod dislocations with line sense; (c) leading Shockley partials with line sense; (d) trailing Shockley partials; and (e) detail of infinitesimal stair rods in between infinitesimal prismatic loops (note that  $b_1 = b_2$ ).

of dislocations and imaging with a weak beam by Carter and Ray<sup>32,33</sup> gave values of 45 mJ/m<sup>2</sup>. The GSF energy evaluated by the *ab initio* method is 46.4 mJ/m<sup>2</sup>, compared with the experimentally measured value<sup>33</sup> of 45 mJ/m<sup>2</sup>.

To deal with the extended core in copper, infinitesimal dislocations representing each segment of the rhombus-shaped loop are classified into two groups, each with different Burgers vectors. The first group is for the leading partial dislocation while the second is for the trailing partial dislocation. Considering the combination of the slip plane and the Burgers vector of partial dislocations, each segment of the extended loop must have a different pair of Burgers vectors for the two infinitesimal partial dislocations. The resulting Burgers vectors for the segments are shown in Fig. 8. Finally, at the corners of each infinitesimal rhombus we ensure that the net Burgers vector is zero by adding a stair-rod dislocation. Figure 8 shows the Burgers vectors and line sense vectors involved in modeling the SIA prismatic loop in copper, wherein (a) the Burgers vector of the full prismatic loop is shown, the stair-rod dislocation with line sense is illustrated in (b), the leading Shockley partials with line sense are shown in (c), the trailing Shockley partials in (d), and finally details of infinitesimal stair rods in between infinitesimal prismatic loops are illustrated in (e). Note that for the leading Shockley partial at the obtuse angle, the Burgers vectors are:  $-\frac{a}{6}[\bar{2}1\bar{1}]$  and  $\frac{a}{6}[\bar{2}11]$ , thus the stair-rod Burgers vector is  $B_{SR}=\frac{a}{3}[001]$ . The stair-rod Burgers vector for the trailing partial at the corresponding node on the trailing partial is the same, but is written as  $\frac{a}{3}[00\bar{1}]$ , because of the line sense reversal at that node. In Fig. 8(e), we give an example of only four infinitesimal SIA loops. In this example, the stair-rod dislocation is divided into four segments, with Burgers vectors determined from the displacement conservation at each node, thus  $b_1=b_a-b_A$ ,  $b_2=b_1+b_a-b_A=2(b_a-b_A)$ ,  $b_3=b_4+b_B-b_b=2(b_B-b_b)$ , and  $b_4=b_B-b_b$ . The corner nodes joining each stair rod with two Shockley partials are allowed to move in the calculations along the stair-rod directions. The initial positions of infinitesimal prismatic loops (and hence the length of each stair rod) is set at uniform intervals, and the force balance equations are solved till equilibrium positions and shapes are obtained. The final dislocation segment positions and shapes are not dependent on the initial positions because they satisfy force equilibrium (and hence minimize the total energy of the system). To determine the dependence of the core structure on the loop size, the core is represented by 20 infinitesimal dislocations and the number of SIAs in each loop is varied as: 16, 100, 400, and 1600.

The GSF energy for copper is calculated using the *ab initio* method<sup>25</sup> for the  $(11\bar{1})$  plane along the  $[\bar{2}1\bar{1}]$  direction, and the results are shown in Fig. 9. Similar to the case of iron, the energy is fitted to a polynomial equation of the form

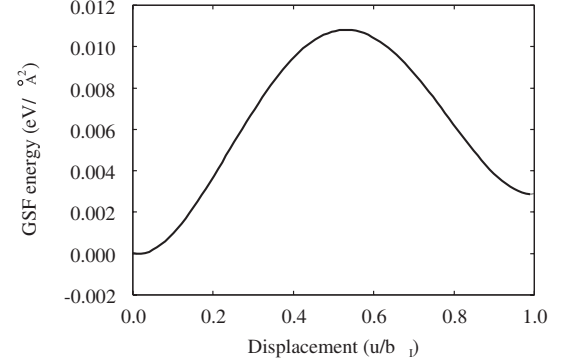


FIG. 9. GSF energy for copper on the  $(11\bar{1})$  plane along the  $[\bar{2}1\bar{1}]$  direction. The displacement is normalized by  $|b_l|=a/\sqrt{6}$ , which is the magnitude of Burgers vector of a Shockley partial dislocation.

$$E_{\text{GSF}} = E_0 + A_1u + A_2u^2 + A_3u^3 + A_4u^4 + A_5u^5 + A_6u^6, \quad (3)$$

where,  $E_0$  and  $A_i$  ( $i=1,6$ ) are the fitting parameters, given in Table I. Note that in Eq. (3),  $u$  is the displacement normalized by the magnitude of the Shockley partial dislocation Burgers vector ( $a/\sqrt{6}$ ). Only half the GSF energy function along the  $A$ - $\gamma$  partial ( $1/6[\bar{2}1\bar{1}]$ ) is fitted to the polynomial function because the shape of the GSF energy is symmetric if we were to continue fitting along the second partial  $\gamma$ - $B$  ( $1/6[\bar{1}21]$ ). The derivative of the GSF energy with respect to  $u$  is then used to calculate the lattice restoring force.

Figure 10 shows the results of the present hybrid simulations. It is noted that infinitesimal dislocation lines, in particular, at the top and bottom of the loop are twisted and expanded for the small self-interstitial loop with 16 SIAs. The concentration of infinitesimal dislocations cannot clearly be seen in the figure, indicating that partial dislocations in small self-interstitial loops have a flat core structure. On the other hand, as the size of the self-interstitial loop increases, the spatial distribution of infinitesimal dislocations acquires two clearly isolated peaks, which delineate fully formed partial dislocations.

Based on the results obtained from the present hybrid model and the atomic configuration reconstruction method described earlier, we will compare here the results of the present model with MD simulations. We performed classical MD simulations of the core structure of an SIA loop containing 100 SIAs with an interatomic potential for copper developed by Mishin *et al.*<sup>32</sup> Similar to the case of iron, an atomic volume with a size of  $7.23 \times 7.23 \times 7.23$  nm<sup>3</sup> is constructed for MD simulations and a rhombus shape of an extra  $\{110\}$  atomic plane with 100 SIAs is inserted at the center. Numerical quenching is first performed to obtain an energetically

TABLE I. Values of the fitting parameters for the GSF energy of copper on the  $(11\bar{1})$  plane along the  $[\bar{2}1\bar{1}]$  direction to the six-order polynomial equation. The units of  $E_0$  and  $A_i$  are (eV/Å<sup>2</sup>).

$E_0$	$A_1$	$A_2$	$A_3$	$A_4$	$A_5$	$A_6$
$1.09504 \times 10^{-5}$	-0.00416	0.16114	-0.24163	-0.02983	0.17648	-0.05913

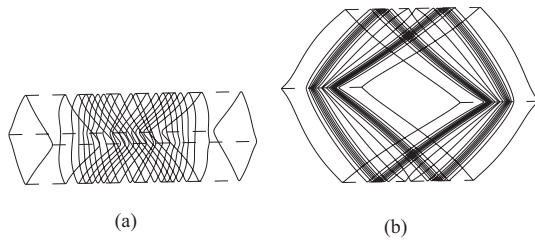


FIG. 10. Core structure of an SIA cluster modeled as a rhomb-shaped edge dislocation loop in copper containing (a) 16 and (b) 400 SIA. Each line represents one infinitesimal dislocation loop and is also considered as an equidisplacement contour line incremented by  $b/20$  ( $\sim 0.006$  nm).

stable structure of the self-interstitial loop. Figure 11 shows the atomic arrangements of the core structure of a cluster containing 100 SIA in copper obtained by MD calculations using the Mishin potential (a and b are compared with those obtained by the present method c and d). The atomic positions shown in Fig. 11 are projected on the (111) plane in a and c, and the  $(\bar{1}10)$  plane in b and d. To show the core structure clearly, atomic positions are analyzed using the central symmetry technique. The results of the analysis are shown in the figure, where gray atoms form the stacking fault, and black atoms surround the partial dislocation core. Comparing the atomic arrangements calculated by classical MD with the results of the present hybrid method clearly shows that the core structure of SIA dislocation loops in

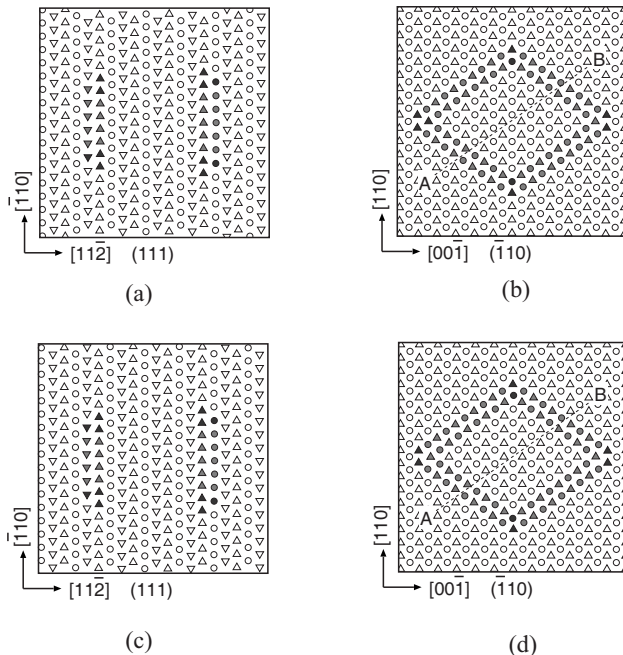


FIG. 11. Atomic arrangements of the core structure of a cluster containing 100 SIA in copper obtained by MD calculations using the Mishin potential (a and b), compared with those obtained by the present method (c and d). The colors are based on the central symmetry technique; gray atoms form the SF, while black atoms surround the partial dislocation core. The atomic positions are projected on the (111) plane (a and c) and the  $\bar{1}10$  plane (b and d).

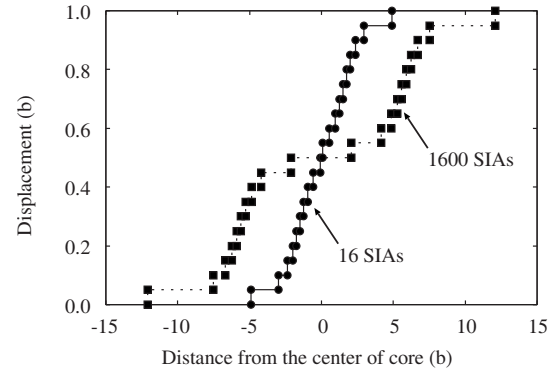


FIG. 12. Displacement distribution of SIA dislocation loop cores in copper for a small cluster containing 16 SIA and for a large cluster containing 1600 SIA.

copper obtained by the present method is indistinguishable from those obtained with MD simulations. In fact, a comparison with Figs. 7 and 8 of Ref. 27, which are obtained by MD simulations using the Ackland potential,<sup>34</sup> shows that the atomic structure obtained by Osetsky *et al.* is also nearly identical to the present results. While the details of atomic arrangements are determined by the dependence of the GSF energy on atomic displacements on the slip plane, the magnitude of the unstable stacking fault energy must be responsible for the degree of dissociation within the core. One advantage of the present method is that the core structure of large dislocation loops can be easily investigated without additional computational difficulties. Moreover, the effects of an applied local stress can also be easily included.

The dependence of the core structure on the size of the SIA loop is then quantitatively studied. Figure 12 shows the displacement distributions within SIA dislocation loop cores in copper for a small cluster containing 16 SIA, and for a large cluster containing 1600 SIA. The figure shows the clear effect of size, where the core of the SIA dislocation loop is more compact for small clusters. In all cases, the displacement distribution is flat in the central part of the dislocation loop core, which corresponds to a stacking fault in the extended dislocation core. However, when the SIA loop contains only 16 SIA, the width of the central region is very narrow, around  $4b$ , indicating that the dislocation core of small SIA loops is only slightly extended, and that the two Shockley partials merge in the center. The width of the shelf, which corresponds to the stacking fault region, becomes larger as the number of SIA in the loop increases. The dependence of the width of the stacking fault on the size of the self-interstitial loop is consistent with the classical MD results of Osetsky *et al.*<sup>27</sup> Figure 13 shows the displacement density within the dislocation core. The figure shows more clearly the structure of the dislocation core such as the width of the stacking fault and the position of Shockley partial dislocations. There are two aspects related to this figure. The first is the displacement density concentration within the partial dislocation core and the second is the width of the stacking fault between the partials. A sharp peak in the displacement density means that partial dislocations are well formed. The stacking fault width is the distance between the partials, and hence the distance between the two peaks of the dis-

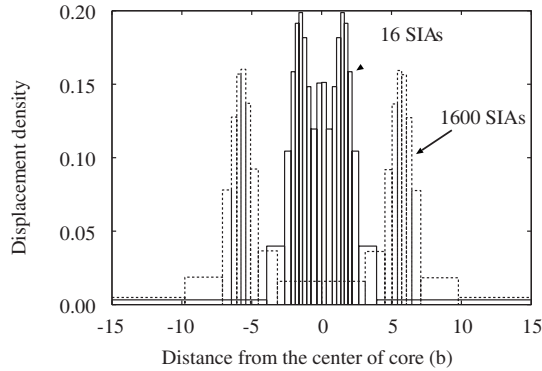


FIG. 13. Displacement density distribution of SIA dislocation loop cores in copper for a small cluster containing 16 SIAs and for a large cluster containing 1600 SIAs.

placement density. The displacement density peaks of the small self-interstitial loop with 16 SIAs are not well separated as compared to peaks observed in larger loops and the separation between them is small, indicating that small SIA loops have a narrow stacking fault region and a flat displacement distribution within the core. As the number of atoms in the SIA loop increases, the width of the stacking fault and the two density peaks become larger, and approaches that of the straight edge dislocation. Note that the SF ribbon width for a straight edge dislocation is  $\sim 14b$ , consistent with the measurements of Carter and Ray.<sup>33</sup> Thus, the current results indicate that the core structure of self-interstitial loops in copper has strong dependence on the size of the loop and that loops with more than  $\sim 400$  SIAs have the same core structure as straight edge dislocations, as can be seen in Fig. 14

#### IV. SIA CLUSTER CORE RESPONSE TO APPLIED SHEAR

Large local stresses, which may result from an externally applied force or internally in the near vicinity of grown-in dislocations, can influence the balance between the various force components holding the SIA cluster together. To determine the effects of the local stress on the core structure, pure shear stress is applied on the slip plane of the rhombus loop

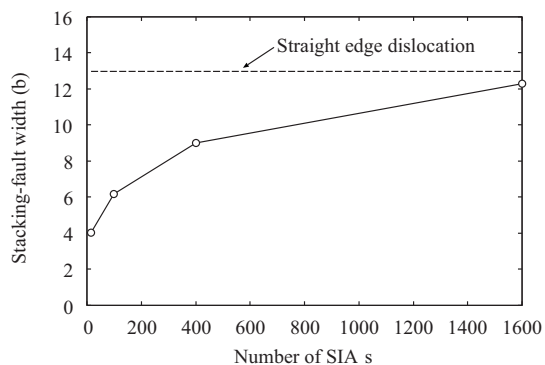


FIG. 14. The dependence of the dislocation core width on the size of the SIA cluster. Results for the SF width of an infinitely long straight edge dislocation are also shown for comparison.

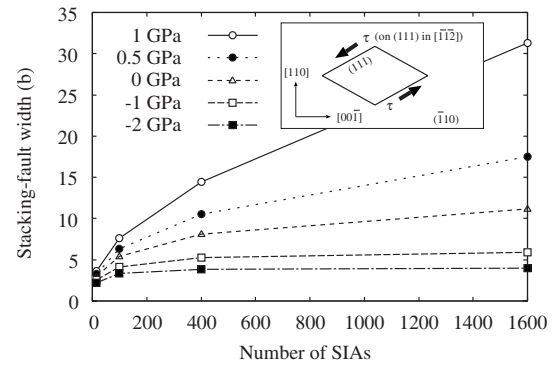


FIG. 15. Dependence of the dislocation core width on (1) the size of SIA cluster and (2) the externally applied shear stress. Positive shear is defined as shown in the inset (on the (111) plane along the  $[\bar{1}\bar{1}2]$  direction). Also, the result without shear stress is added as reference.

edges along the  $[\bar{1}\bar{1}2]$  direction with a positive sense as shown in the inset of Fig. 15. The figure also shows the dependence of the stacking fault width on the number of SIAs within the cluster for positive and negative applied shear, and the unstressed case is also included for comparison. The edge component of the Burgers vector of the rhombus loop edges has no reaction with the shear stress, while the reaction of the screw component with the shear stress results in the movement of the rhombus loop partials. If the shear stress is positive, the leading and trailing partials move away from one another, and the stacking fault between the partials is widened. The opposite takes place for a negative value of the shear stress. It is interesting to see that negative shear renders the core more compact, and nearly independent of size for sizes larger than approximately 400 SIAs. On the other hand, large positive shear delocalizes the core of the SIA cluster, and for a large-enough shear stress and a size larger than  $\sim 600$  SIAs, the cluster core is totally delocalized. The compressive state within the core becomes nonlocal and of a long-range nature. These results highlight the need to consider the influence of the local stress state on the atomic structure, and hence on the elastic interactions between SIA clusters and other defects.

#### V. SUMMARY AND CONCLUSIONS

The extended Peierls-Nabarro model that describes atomic displacement distributions within a dislocation core has been further developed to determine the core structure of self-interstitial atom clusters in both iron (bcc) and copper (fcc). The distinct aspects of the present development include *ab initio* determination of the resistance to slip on the slip planes of dislocation loop segments comprising the SIA cluster, representation of curved dislocation segments in complex geometry, and the development of a method to reconstruct atomic configurations for direct comparisons with MD simulations. The use of infinitesimal dislocations to describe the core structure in the hybrid method eliminates the singularity of the dislocation core in the elasticity solution, enabling determination of the atomic displacements around the dislo-



cation core on the basis of elasticity theory. Atomic arrangements are reconstructed by elastically displacing atoms from their equilibrium positions. These developments open the door to studies of complex defect structures without recourse and reliance on empirical interatomic potentials. In addition, the simulation volume of the hybrid method can be substantially larger than any corresponding MD simulation volume, because the calculations are performed only for the defect contents and not for all atoms, as is typical in MD simulations. An additional advantage is that the local chemistry effects on defects (such as afforded by the presence of impurities or gas atoms) can be incorporated once the influence of the impurities on the slip resistance is determined from *ab initio* calculations.

We summarize here the main physical results of the present work on the core structure of SIA atom clusters in iron and copper: (1) the core structure of self-interstitial loops in iron is very compact and has no clear dependence on the dislocation loop size. The core structure is nearly identical to that of a straight edge dislocation in iron. (2) Atomic arrangements within the core of SIA clusters in iron are in excellent agreement with classical MD simulations utilizing the Ackland and Mendelev interatomic potentials. The agreement is a consequence of the large unstable stacking fault energy in iron, forcing core atoms to be in compact configurations. (3) The core structure of self-interstitial loops in copper is extended into a combination of a stacking fault and Shockley partial dislocations. The core structure is shown to have a strong dependence on the size of the loop. Small self-interstitial loops have narrow stacking fault regions, on

the order of  $4b$ , and their core displacement distribution is flat, indicating that partials are not well formed and that they merge in small clusters. On the other hand, as the size of the self-interstitial loop increases, the width of the stacking fault and the displacement density concentrated in partial dislocations become larger. (4) The core structure of the self-interstitial loops in copper with more than  $\sim 400$  SIAs is almost the same as that of the straight edge dislocation. (5) Atomic arrangements in copper calculated by the classical MD method are dependent on the interatomic potential used. Good agreement is obtained between the present hybrid method and the MD calculations of Osetsky using the Ackland potential. (6) An applied external shear can delocalize the core of an SIA cluster in copper, with positive shear defined to be on the (111) plane along the  $[\bar{1}\bar{1}2]$  direction. For an SIA cluster containing 1600 atoms, a positive 1 GPa shear stress delocalizes the cluster and expands the SF to  $30b$ , while a negative shear stress of 2 GPa contracts the core to less than  $5b$ , where  $b$  is the Burgers vector magnitude.

#### ACKNOWLEDGMENTS

The authors would like to acknowledge the assistance of Benjamin Ramirez with *ab initio* calculations, and discussions with D. Bacon and Y. Osetsky on the stair-rod dislocation in Cu. This work is supported by the U.S. Department of Energy, Office of Nuclear Energy through Grant No. DE-FC07-06ID14748, and the Office of Fusion Energy through Grant No. DE-FG02-03ER54708 with UCLA.

- 
- <sup>1</sup>T. D. de la Rubia, R. Averback, H. Hsieh, and R. Benedek, *J. Mater. Res.* **4**, 579 (1989).  
<sup>2</sup>T. Diaz de la Rubia and M. W. Guinan, *Phys. Rev. Lett.* **66**, 2766 (1991).  
<sup>3</sup>Y. Osetsky, D. Bacon, Z. Rong, and B. Singh, *Philos. Mag. Lett.* **84**, 745 (2004).  
<sup>4</sup>D. Walgraef, J. Lauzeral, and N. M. Ghoniem, *Phys. Rev. B* **53**, 14782 (1996).  
<sup>5</sup>W. Jaeger, P. Ehrhart, and W. Schilling, in *Nonlinear Phenomena in Materials Science*, edited by G. Martin and L. Kubin (Trans Tech, Aedermannsdorf, Switzerland, 1988), p. 279.  
<sup>6</sup>N. Ghoniem and D. Walgraef, *Modell. Simul. Mater. Sci. Eng.* **1**, 569 (1993).  
<sup>7</sup>H. Trinkaus, B. N. Singh, and S. I. Golubov, *J. Nucl. Mater.* **283-287**, 89 (2000).  
<sup>8</sup>B. Singh, A. Foreman, and H. Trinkaus, *J. Nucl. Mater.* **249**, 103 (1997).  
<sup>9</sup>H. Trinkaus, B. Singh, and A. Foreman, *J. Nucl. Mater.* **249**, 91 (1997).  
<sup>10</sup>N. Ghoniem, S.-H. Tong, B. Singh, and L. Sun, *Philos. Mag. A* **81**, 2743 (2001).  
<sup>11</sup>M. Wen, N. Ghoniem, and B. Singh, *Philos. Mag.* **85**, 2561 (2005).  
<sup>12</sup>D. Bacon, Y. Osetsky, and Z. Rong, *Philos. Mag.* **86**, 3921 (2006).  
<sup>13</sup>V. V. Bulatov, O. Richmond, and M. Glazov, *Acta Mater.* **47**, 3507 (1999).  
<sup>14</sup>M. S. Duesbery, *Dislocations in Solids* (North-Holland, Amsterdam, 1989), Vol. 8, p. 67.  
<sup>15</sup>M. J. Mills, M. S. Daw, and S. M. Foiles, *Ultramicroscopy* **56**, 79 (1994).  
<sup>16</sup>C. Domain and C. S. Becquart, *Phys. Rev. B* **65**, 024103 (2001).  
<sup>17</sup>C. Domain, C. S. Becquart, and J. Foct, *Phys. Rev. B* **69**, 144112 (2004).  
<sup>18</sup>F. Nabarro, *Proc. Phys. Soc.* **59**, 256 (1947).  
<sup>19</sup>S. Banerjee, N. Ghoniem, G. Lu, and N. Kioussis, *Philos. Mag.* **87**, 4131 (2007).  
<sup>20</sup>N. Ghoniem, *ASME J. Eng. Mater. Technol.* **121**, 136 (1999).  
<sup>21</sup>N. M. Ghoniem, S.-H. Tong, and L. Z. Sun, *Phys. Rev. B* **61**, 913 (2000).  
<sup>22</sup>V. Vitek, *Philos. Mag.* **18**, 773 (1968).  
<sup>23</sup>M. Shehadeh, G. Lu, S. Banerjee, N. Kioussis, and N. Ghoniem, *Philos. Mag.* **87**, 1513 (2007).  
<sup>24</sup>G. Lu, N. Kioussis, V. V. Bulatov, and E. Kaxiras, *Phys. Rev. B* **62**, 3099 (2000).  
<sup>25</sup>J. Hafner, *Vienna Ab-initio Package Simulation* (VASP, University of Vienna, Vienna, Austria, 2008).  
<sup>26</sup>N. M. Ghoniem and L. Z. Sun, *Phys. Rev. B* **60**, 128 (1999).  
<sup>27</sup>Y. Osetsky, A. Serra, B. Singh, and S. Golubov, *Philos. Mag. A* **80**, 2131 (2000).

- <sup>28</sup>E. Kuramoto, K. Ohsawa, J. Imai, K. Obata, and T. Tsutsumi, *J. Nucl. Mater.* **329-333**, 1223 (2004).
- <sup>29</sup>M. Finnis and J. Sinclair, *Philos. Mag. A* **50**, 45 (1984).
- <sup>30</sup>M. I. Mendelev, S. Han, D. J. Srolovitz, G. J. Ackland, D. Y Sun, and M. Asta, *Philos. Mag.* **83**, 3977 (2003).
- <sup>31</sup>C. S. Pande, *Phys. Status Solidi B* **37**, 151 (1970).
- <sup>32</sup>Y. Mishin, M. J. Mehl, D. A. Papaconstantopoulos, A. F. Voter, and J. D. Kress, *Phys. Rev. B* **63**, 224106 (2001).
- <sup>33</sup>C. Carter and I. Ray, *Philos. Mag.* **35**, 189 (1977).
- <sup>34</sup>G. Ackland, G. Tichy, V. Vitek, and M. Finnis, *Philos. Mag. A* **56**, 735 (1987).